COMPARISON OF JET-INDUCED LIFT LOSS FOR SINGLE AND CO-ANNULAR JETS

A J Saddington & K Knowles
Aeromechanical Systems Group
Cranfield University, RMCS, Shrivenham
Swindon, SN6 8LA, UK

Keywords: *jet, co-annular, STOVL, suckdown*

Abstract

A series of experiments has been conducted to measure the suckdown force induced on a circular flat baffle plate by a co-annular jet operating in ground effect. A range of nozzle pressure ratio (NPR) and height combinations was investigated. Total pressure measurements were also made using a Pitot probe traversed radially through the centre of the jet and along the jet axis.

Total pressure traverses through the jet centre indicated that the co-annular jet had reasonably good axi-symmetry. The data agreed quite well with previous experimental observations regarding decay rates and core acceleration in some inverted-profile cases. With a subsonic core flow, suckdown force measurements in ground effect were largely independent of NPR. With a supersonic core flow, the results indicated that a normal profile co-annular jet gave a lower percentage suckdown at nozzle heights $h/D < 5$. All the data showed good correlation with previous experiments.

Nomenclature

A_n	total nozzle area [1958.73] (mm^2)
C_p	pressure coefficient $\left\{\frac{p-p_\infty}{\frac{1}{2}(P_a+P_c)-p_\infty}\right\}$
d_a	annular stream nozzle inner diameter [35.81] (mm)
d_c	core stream nozzle diameter [35.33] (mm)
d_{ne}	equivalent nozzle diameter $2\sqrt{\frac{A_n}{\pi}}$ (mm)
D	annular stream nozzle outer diameter [50.28] (mm)
D_p	baffle plate diameter [500] (mm)
F	thrust (N)
h	height above the impingement plate (mm)
ΔL	suckdown force in ground effect (N)
ΔL_∞	suckdown force out of ground effect (N)
M	Mach number
NPR	nozzle pressure ratio $\left\{\frac{P}{p_\infty}\right\}$
p	static pressure (Pa)
P	total pressure (Pa)
$\mathrm{Per}_{\mathrm{total}}$	total nozzle perimeter $\{\pi D\}$ (mm)
S	baffle plate area [1.9635×10^5] (mm^2)
T	temperature (K)
x, y, z	Cartesian co-ordinates (mm). The origin is at the centre of the nozzle exit plane. The x-direction represents the traverse table movement. The y-direction represents the probe movement (the probe entering from the negative y-direction). The z-direction represents the vertical distance from the nozzle exit plane. The jet is orientated with its efflux in the negative z-direction.
γ	ratio of specific heats [1.4]

Subscripts

1	conditions upstream of a normal shock wave
2	conditions downstream of a normal shock wave
a	annular nozzle conditions
c	core nozzle conditions
∞	ambient conditions

1 Introduction

The development of short take-off and vertical landing (STOVL) military aircraft has been an attractive goal for many governments and aircraft companies all over the world, especially in Europe and the USA. Through the Joint Strike Fighter (JSF) programme, research is continuing in the UK and USA with the aim of developing a new generation of STOVL fighter aircraft. The STOVL version of the JSF is intended to replace Royal Navy Sea Harrier FRS-2s, RAF Harrier GR7s and US Marine Corps AV-8Bs.

1.1 Background

STOVL aircraft introduce many aerodynamic characteristics unique to their operation. The flow-fields surrounding such aircraft, during hover and during transition from hover to wing-borne flight, are of particular importance. In hover, high velocity fluid from the direct lift system mixes with ambient air to form an entrainment flow-field. The entrainment flow-field causes a download on the airframe (known as 'suckdown') which effectively reduces the thrust of the lift system. Out of ground effect (greater than 50 nozzle diameters or so, above the ground) the suckdown may be quite small, of the order of 1% to 2% of thrust. As the aircraft moves into ground effect, however, the suckdown increases rapidly with reducing altitude. Numerous studies have been carried out in the past on the suckdown generated by a single circular jet issuing from a flat plate e.g. references [1] to [11].

A successful JSF design will require a novel propulsion system to enable the aircraft to meet stringent performance criteria. The use of a fan, either shaft driven or gas driven, as well as a dedicated lift jet engine have been proposed for the forward lift post in these aircraft. All of these designs result in a co-annular jet issuing from the forward fuselage. A normal velocity profile (i.e. one where the core pressure ratio is higher than the annular) would be produced by a lift jet whereas an inverted velocity profile (i.e. one where the core pressure ratio is lower than the annular) would be produced by a lift fan.

1.2 Aim

Kirkham[12] and Knowles & Kirkham[13] summarise previous works on co-annular jets, which have concentrated on examining the jet structure and recording flow properties within the jet. There appears to be no previous work on the effect co-annular jets have on suckdown.

In co-operation with DERA (Bedford) a short study was instigated using a co-annular nozzle system. The aim of the study was to determine jet-induced suckdown forces on a circular flat plate, in ground effect, over a range of jet conditions.

2 Co-annular Jet Package

Fig. 1 shows the two co-annular nozzles with the core nozzle on the left. The nozzles are of the truncated Stratford type (i.e. with no divergent section), the design of which is described by Kirkham[12]. Each air stream, designated annular and core, had nominally identical nozzle exit areas of 9.79×10^{-4} m^2. The principle nozzle dimensions are as follows:

- D = 50.28 mm;
- d_a = 35.81 mm;
- d_c = 35.33 mm.

The co-annular jet package was installed in the DERA (Bedford) impinging jet test cell (Fig. 2). The Pitot probe, which was used to measure total pressure profiles, is seen in position below the nozzle exit. In the bottom right of the picture is the spark/continuous light source and 35 mm stills camera, which were used to record shadowgraph images. There is also a miniature CCD camera which was used to record video footage of the tests.

3 Experimentation

Two sets of data were recorded. These were designated Configuration 1 and Configuration 2.

3.1 Configuration 1

Configuration 1 consisted of a series of total pressure measurements. A Pitot probe was traversed through the jet (Fig. 3), in either the x or y direction, at a series of distances z downstream from the nozzle exit. In addition, a 2d area trav-

erse was carried out at NPR_a = 1.5, NPR_c = 1.0, z/D = -0.994. Some centre-line total pressure measurements were also made.

3.2 Configuration 2

Configuration 2 consisted of a series of suck-down measurements. A flat circular baffle plate of 500 mm diameter was installed around the nozzle (Fig. 4) such that the lower surface of the plate and the nozzle exit plane were co-planar. The baffle plate was mounted 'live' to three load cells which measured the suckdown force on the plate when the jet was operational. By subtracting the force on the plate with the jet efflux switched off, the net suckdown force on the plate could be determined.

To enable the effect of ground proximity to be assessed, a 2 m by 2 m ground board was positioned below the nozzle, and a 1 m diameter, 12.7 mm thick impingement plate was mounted onto the ground board (Fig. 4). The suckdown force in ground effect was recorded for a number of NPR and height combinations which are summarised in Table 1.

3.3 Calibration of the Co-annular Jet Package

Calibration of the Co-annular Jet Package was carried out by the Aircraft Research Association (ARA) following the completion of the tests described above. The aim of the calibration was to determine the co-annular nozzle thrust over a range of core and annular NPR combinations. Further details are presented in the calibration report[14].

4 Results

Results are presented for the tests on the two configurations described in Section 3.

4.1 Configuration 1

4.1.1 1-d Total Pressure Traverses

Pitot probe data was collected for traverses made in the x and y directions through the jet centre for various combinations of NPR and probe height. For NPRs greater than 1.893 (in isentropic air flow) a bow shock will form in front of the Pitot probe giving an error in the measured total pressure. This error is given by the ratio of total pressures across a normal shock wave

$$\frac{P_2}{P_1} = \left[\frac{\frac{1}{2}(\gamma+1)M_1^{\,2}}{1+\frac{1}{2}(\gamma-1)M_1^{\,2}}\right]^{\frac{\gamma}{\gamma-1}} \left[\frac{2\gamma}{\gamma+1}M_1^{\,2} - \frac{\gamma-1}{\gamma+1}\right]^{\frac{1}{1-\gamma}} \quad (1)$$

If we assume that the upstream Mach number is that given by an ideally expanded jet, then the ratio of total pressures across the shock wave can be determined. For an NPR of 3.5, the highest tested, the ratio is 0.94:1 i.e. the downstream total pressure is 94% of the upstream but is closer to 100% for lower NPRs. In reality the upstream Mach number may be less than that produced by an ideally expanded jet. This is due to the underexpanded convergent nozzle producing a higher than ambient static pressure at exit. This will result in a total pressure ratio closer to unity. The complexity of the flow field close to the nozzle exit and the lack of any additional data renders error correction of this nature difficult and somewhat speculative. As a consequence, no attempt has been made to correct the recorded total pressures for Pitot probe bow shock effects.

An extensive range of profiles were recorded for the annular jet of NPR_a = 1.5, NPR_c = 1.0 (Fig. 5). The decay of the annular jet profile into a normal profile (i.e. highest pressure in the centre) can clearly be seen. The results show good agreement with Knowles & Kirkham[13] in terms of the velocity profile shape. Direct comparisons are difficult due to the different nozzle operating conditions. The pressure profile measurements in this study were too coarse to determine the length of the potential core for this annular nozzle flow although it is clear that it has already decayed by z/D = -2.

For the profiles which included an x and y traverse at the same height (e.g. Fig. 6) reasonably good symmetry is seen. Some of the normal and equal NPR co-annular jet profiles (e.g. Fig. 7 and Fig. 8) exhibited non-uniform total pressure profiles close to nozzle exit. In the case of Fig. 7 there is a total pressure deficit on the jet centre line and in the case of Fig. 8 there is a total pressure peak on the jet centre line. It is not

known whether the non-uniform exit profile is genuine or whether these effects are a result of the Pitot probe traversing through the shock structure of the jet which gives an apparent non-uniformity to the jet flow close to nozzle exit. In the case of Fig. 7 (NPR_a = 1.5, NPR_c = 2.5) the centre-line total pressure profile does show evidence of a shock structure which is seen as a fall and rise in total pressure as the core jet expands to atmospheric pressure (Fig. 9).

Fig. 10 shows three traverses for an inverted profile jet (NPR_a = 2.5, NPR_c = 1.5) which indicate that the potential core for the core nozzle extends to z/D = -4. At this downstream distance the co-annular flow is still evident. With higher NPRs in both annular and core nozzles (NPR_a = 3.0, NPR_c = 2.5) the potential core in the core flow extends beyond z/D = -4 (Fig. 11) but the co-annular flow has decayed by this point.

With a high NPR annular jet (NPR_a = 3.5) one might expect the annular jet to decay quite slowly but this is not the case (Fig. 12). This may be due to the fact that the annular jet is able to spread both inwards as well as outwards and hence its decay rate is increased. Fig. 12 shows that the annular flow has decayed by z/D = -4. With the same annular flow conditions (NPR_a = 3.5) and the addition of some core flow (NPR_c = 1.5), the annular flow is still evident at z/D = -4 (Fig. 13). The decay rate of the co-annular and core flows is, therefore, dependent on the relative magnitude of the NPRs as well as the magnitudes themselves.

Knowles & Kirkham[13] found the core nozzle potential core length to be about 4 d_c (z/D = -2.6) for NPR_c = 1.3, NPR_a = 2.2 and about 8 d_c (z/D = -5.3) for almost choking core nozzles (NPR_c = 1.8, NPR_a = 2.2). The present data agree quite well with these results and are consistent with the findings of Curtis[15] who suggests that subsonic potential core length increases with NPR. Curtis's supporting data for this conclusion is, however, quite limited. Knowles & Kirkham[13] also reported an acceleration of the core flow for inverted profiles if the core were sub-critical. This is also seen here, as in Fig. 5, Fig. 12 and Fig. 13. Such behaviour might also be expected in Fig. 10 if traverses had been taken further downstream.

4.1.2 2-d Total Pressure Area Traverse

At one nozzle condition (NPR_a = 1.5, NPR_c = 1.0) a total pressure area traverse was made (Fig. 14). The figure shows contours of local pressure ratio at an axial distance z/D = -0.994 below the jet exit plane. The jet exhibits fairly good axial symmetry although there does appear to be some flattening of the contours which may be due to the resolution of the measurements. Other asymmetries may be due to probe stem interference as the probe penetrates the jet.

The extremities of the core and annular nozzles are shown by the black circles. It is clear that at only 1 annular nozzle diameter downstream from the exit plane the annular jet has contracted inwards quite considerably, the maximum total pressure region having moved well within the core nozzle area. It should be noted, however, that there is no core nozzle flow in this case, other than that induced by the annular jet. Fig. 5 presents profiles through the jet centre-line at this and downstream locations.

4.2 Configuration 2

Fig. 15, Fig. 16, Fig. 17 and Fig. 18 show the jet-induced suckdown in ground effect for a range of nozzle height and NPR combinations. As can be seen, suckdown increases exponentially with reducing nozzle height and gives very high suckdown forces at h/D<3. In cases with a subsonic core flow (Fig. 15 and Fig. 16) there is no identifiable trend in suckdown with variations in annular NPR. It does appear that in some instances a high NPR annular flow is slightly beneficial (e.g. h/D=4 in Fig. 15). With a wholly supersonic core flow (Fig. 17 and Fig. 18), there appears to be some benefits in having a low NPR annular flow. Per cent suckdown decreases with reducing annular jet NPR particularly at heights h/D<5.

Empirical correlations exist which link the jet-induced suckdown force to the nozzle height. Two such correlations are given by Wyatt[1]:

$$\frac{\Delta L - \Delta L_\infty}{F} = 0.012\left(\frac{h}{D_p - D}\right)^{-2.3} \qquad (2)$$

and Corsiglia *et al* [9]:

$$\frac{\Delta L - \Delta L_\infty}{F} = 0.016\left(\frac{h}{D_p - D}\right)^{-2.38} \quad (3)$$

Fig. 19 shows the two correlations plotted against the recorded co-annular nozzle data. The data generally agree well with the correlations, particularly that of Corsiglia. The discrepancy between Wyatt's and Corsiglia's correlations (known as the Wyatt anomaly) was the subject of protracted debate but has recently been explained by Clark & Murgatroyd[10] and subsequently published by Ing & Zhang[11]. The discrepancy is due to baffle plate edge geometry. In the case of Wyatt it was square and in the case of Corsiglia chamfered (as was the plate in the tests described here). For the co-annular configuration tested, the data best fit the equation

$$\frac{\Delta L - \Delta L_\infty}{F} = 0.025\left(\frac{h}{D_p - D}\right)^{-2.02} \quad (4)$$

These correlations do not, however, include the effect of NPR or exit velocity profile.

The in ground effect data was separated into three categories; equal-NPR, normal-profile and inverted-profile. These are shown in Fig. 20, Fig. 21 and Fig. 22 respectively. The equal-NPR jet data (Fig. 20) show very little scatter and agree quite well with Corsiglia's correlation although the slopes differ. The normal-profile jet data (Fig. 21) have more scatter but again agree well with Corsiglia's correlation. The inverted-profile data (Fig. 22) also agree well, again the slope of the data differing slightly from the slope of Corsiglia's correlation.

5 Conclusions

The main conclusions which can be drawn from this co-annular jet study are as follows.

- Total pressure traverses through the jet centre indicated that the co-annular jet had reasonably good axi-symmetry. The data agreed quite well with the observations of Knowles & Kirkham[13] regarding decay rates and core acceleration in some inverted-profile cases. It may be concluded, therefore, that the findings of Knowles and Kirkham[13] apply equally well to the co-annular jets in the present study.
- With a subsonic core flow, suckdown force measurements in ground effect were largely independent of NPR. With a supersonic core flow, the results indicated that a normal profile co-annular jet gave a lower percentage suckdown at nozzle heights $h/D<5$. All the data showed good correlation with previous experiments. An equation linking suckdown force with nozzle height was proposed (Eqn. 4).

6 Acknowledgements

This work was funded by the MoD under package 7b of the Applied Research Programme and under contract to Cranfield University through university agreement number ASF/3237U. The authors wish to express their thanks to Mr Bob Clark of DERA (Bedford) for his advice and assistance throughout the project.

7 References

[1] WYATT, L. A., Static Tests of Ground Effect on Planforms Fitted with a Centrally-located Round Lifting Jet, *Aeronautical Research Council*, C.P. No. 749, 1964.

[2] KUHN, R. E. & MCKINNEY, M. O. JR., NASA Research on the Aerodynamics of Jet VTOL Engine Installations, *AGARDograph 103*, Specialists Meeting, Tennessee, USA, pp. 689-713, 25-27 October, 1965.

[3] GENTRY, G. L. JR. & MARGASON, R. J., Jet-induced Lift Losses on VTOL Configurations Hovering In and Out of Ground Effect, *NASA Technical Note TN D-3166*, 1966.

[4] HAMMOND, A. D., Thrust Losses in Hovering for Jet VTOL Aircraft, *NASA Special Proceedings SP-116*, pp. 163-175, 1966.

[5] MCLEMORE, H. C., Jet-induced Lift Loss of Jet VTOL Configurations in Hovering Condition, *NASA Technical Note TN D-3435*, 1966.

[6] WILLIAMS, J. & WOOD, M. N., Aerodynamic Interference Effects With Jet-lift V/STOL Aircraft Under Static and Forward Speed Conditions, *RAE Technical Report No. 66403*, 1966.

[7] SHUMPERT, P. K. & TIBBETTS, J. G., Model Tests of Jet-induced Lift Effects on a VTOL Aircraft in Hover, *NASA Contractor Report CR-1297*, 1969.

[8] BRADBURY, L. J. S., Some Aspects of Jet Dynamics and Their Implications for VTOL Research, *AGARD Conference Proceedings CP-308*, Fluid Dynamics Panel Symposium, Fundaçao Calouste Gulbenkian, Lisbon, Portugal, pp. 1.1-1.26, 2-5 November, 1981.

[9] CORSIGLIA, V. R., WARDWELL, D. A. & KUHN, R. E., Small-scale Experiments in STOVL Ground Effects, *Proceedings of the International Powered Lift Conference*, London, UK, pp. III.14.1-III.14.13, 29-31 August, 1990.

[10] CLARK, R. & MURGATROYD, J. D., Ground-effect Lift Loss Due to Single Jet Impingement: the 'Wyatt anomaly', *Defence Research Agency Report No. DRA/AS/AP/CR93012/1*, November 1993.

[11] ING, D. N. & ZHANG, X., An Experimental and Computational Investigation of Ground Effect Lift Loss for Single Jet Impingement, *RAeS Aeronautical Journal*, Vol. 98, No. 974, pp. 127-136, 1994.

[12] KIRKHAM, L., Coaxial Jet Flows For ASTOVL Applications, *MPhil Thesis*, Cranfield University, 1996.

[13] KNOWLES, K. & KIRKHAM L., Inverted-profile Coaxial Jet Flows Relevant to ASTOVL Applications, *The RAeS Aeronautical Journal*, pp. 377-384, August/September 1998.

[14] ELLIOTT, M., Calibration of a Co-annular Jet Flow Package in the ARA MST1 Facility, *ARA Contractor Report M346/2*, 1999.

[15] CURTIS P., Investigation Into the Behaviour of a Single Jet in Free Air and Impinging Perpendicularly on the Ground, *BAe Report No. BAe-KAD-R-RES-3349*, September 1987.

Tables

NPR_a	NPR_c	h/D
1.5	1.0	2 to 10
2.5	1.0	2 to 10
3.5	1.0	2 to 10
1.0	1.5	1.4 to 7
1.5	1.5	2 to 10
2.5	1.5	2 to 10
3.5	1.5	2.3 to 10
1.0	2.5	1.6 to 7
1.5	2.5	2 to 10
2.5	2.5	2 to 10
3.5	2.5	2.6 to 10
1.0	3.5	2 to 10
1.5	3.5	2 to 10
2.5	3.5	2.4 to 10
3.5	3.5	2.8 to 10

Table 1. In ground effect test matrix.

Figures

Fig. 1. Co-annular nozzles in isolation.

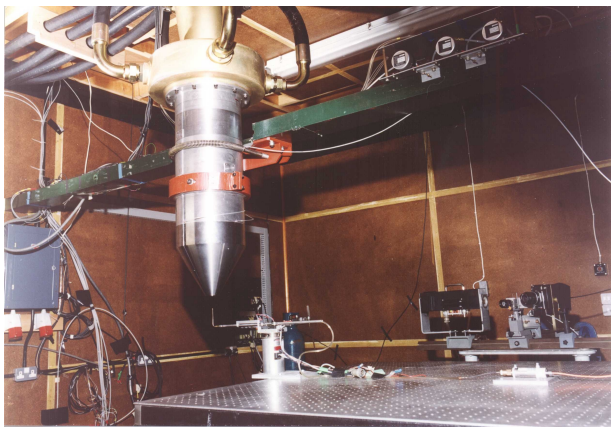

Fig. 2. Co-annular jet package installed in the test cell.

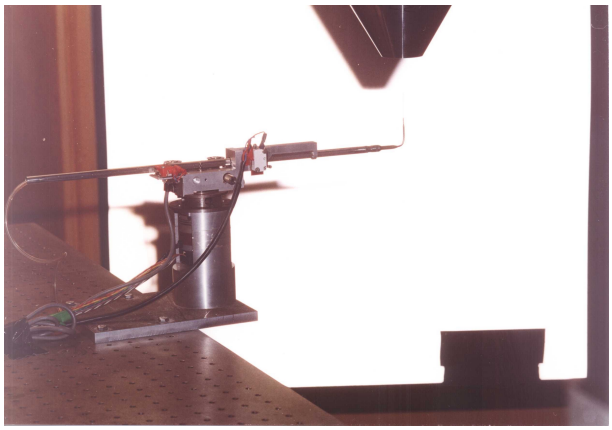

Fig. 3. Traverse-mounted Pitot probe.

Fig. 4. Co-annular jet package in ground effect.

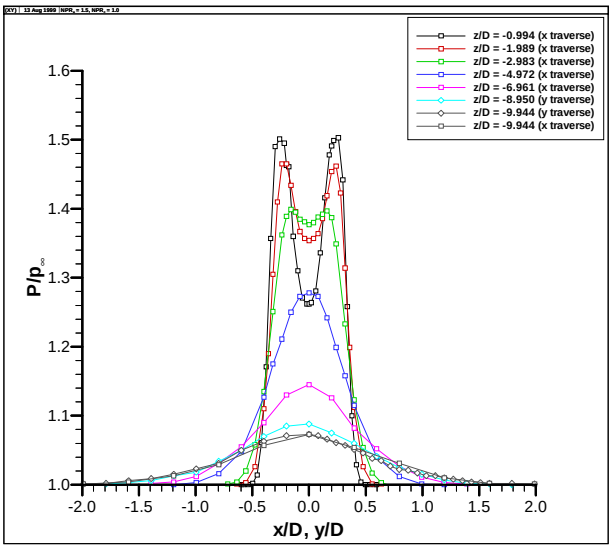

Fig. 5. Pitot pressure traverse (NPR_a = 1.5, NPR_c = 1.0).

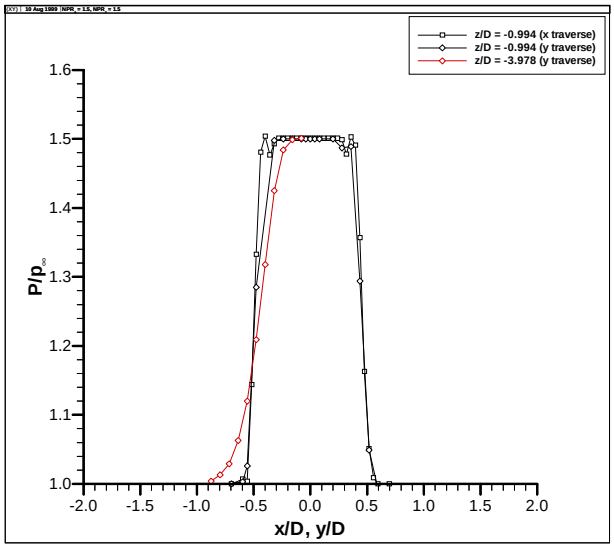

Fig. 6. Pitot pressure traverse (NPR_a = 1.5, NPR_c = 1.5).

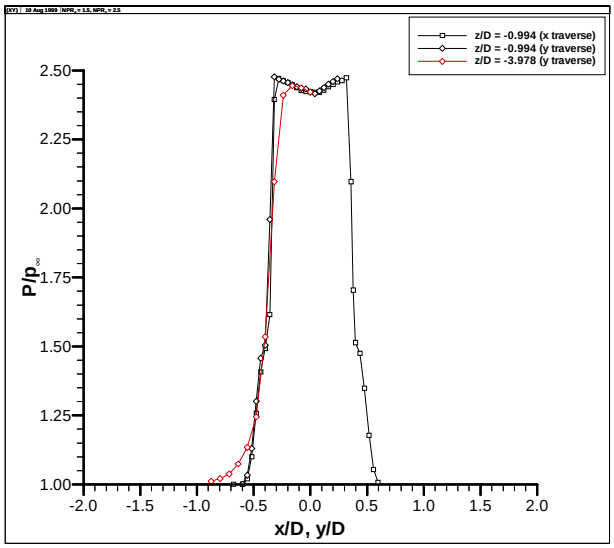

Fig. 7. Pitot pressure traverse (NPR_a = 1.5, NPR_c = 2.5).

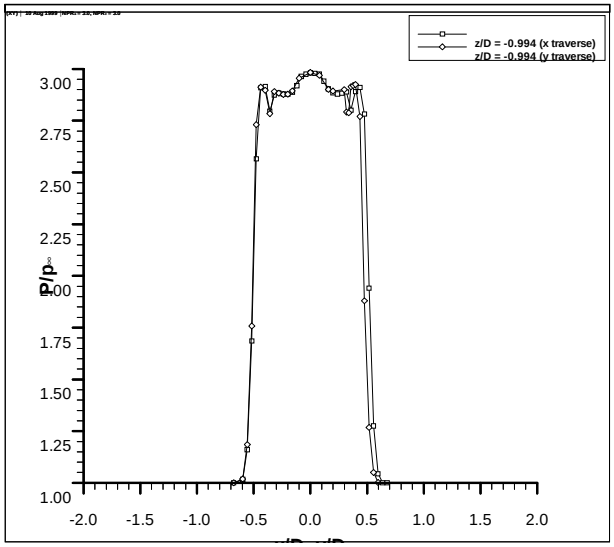

Fig. 8. Pitot pressure traverse (NPR_a = 3.0, NPR_c = 3.0).

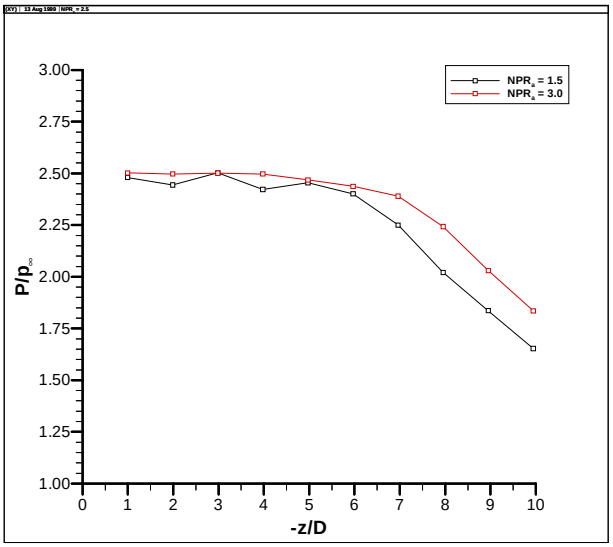

Fig. 9. Centre-line Pitot pressure profiles (NPR$_c$ = 2.5).

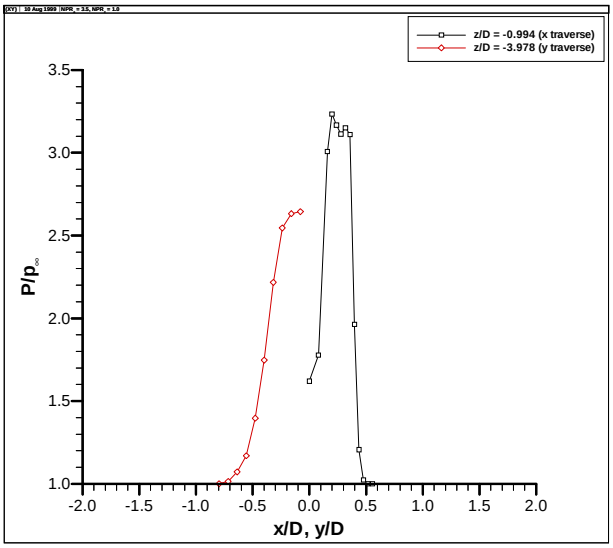

Fig. 12. Pitot pressure traverse (NPR$_a$ = 3.5, NPR$_c$ = 1.0).

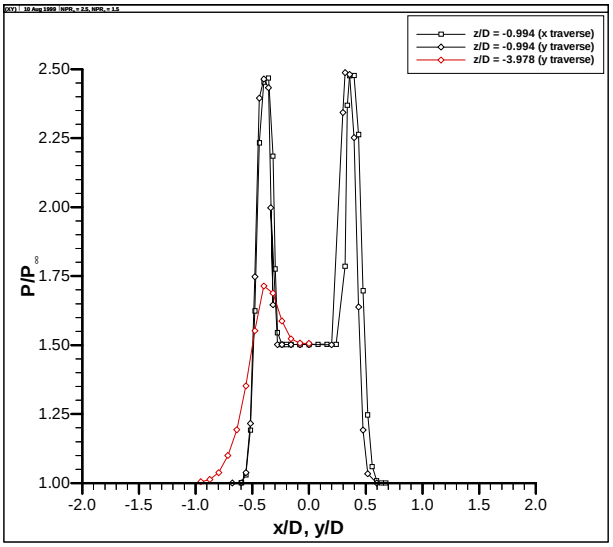

Fig. 10. Pitot pressure traverse (NPR$_a$ = 2.5, NPR$_c$ = 1.5).

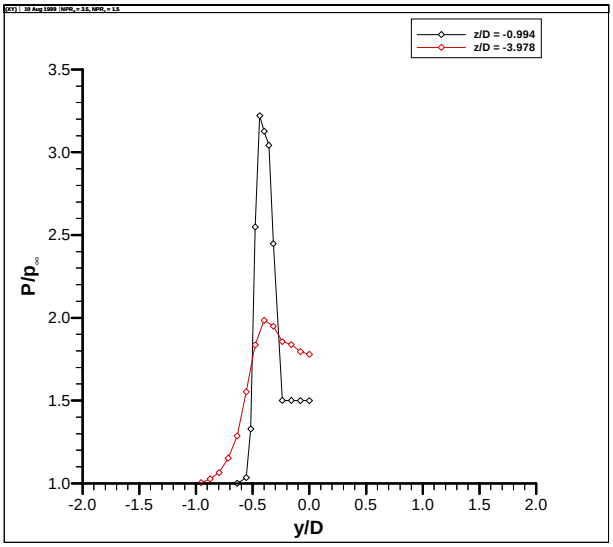

Fig. 13. Pitot pressure traverse (NPR$_a$ = 3.5, NPR$_c$ = 1.5).

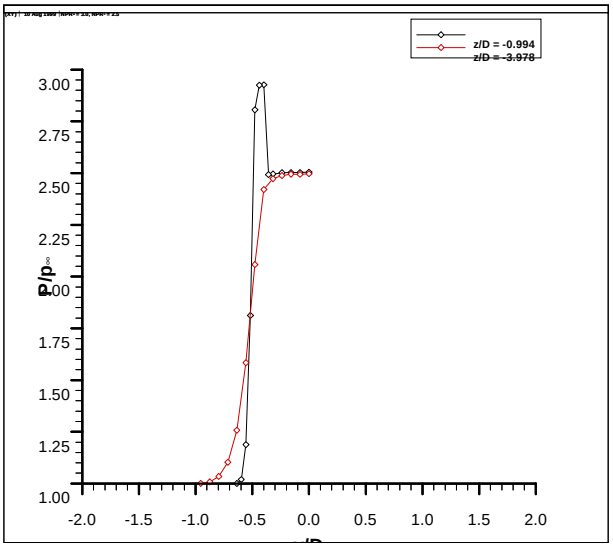

Fig. 11. Pitot pressure traverse (NPR$_a$ = 3.0, NPR$_c$ = 2.5).

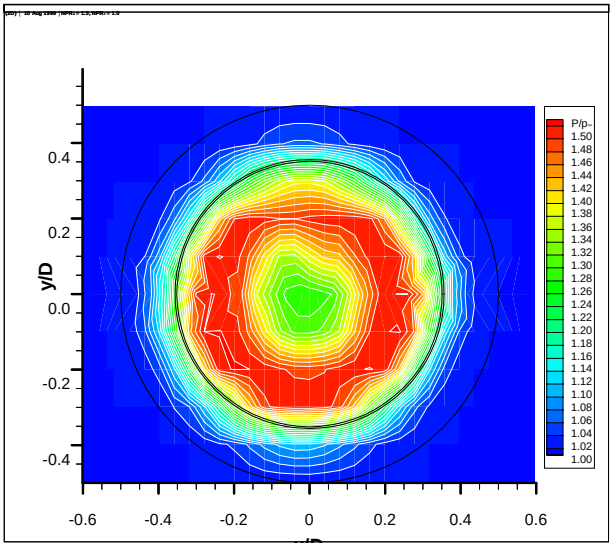

Fig. 14. Pitot pressure area traverse (NPR$_a$ = 1.5, NPR$_c$ = 1.0, *z/D* = -0.994).

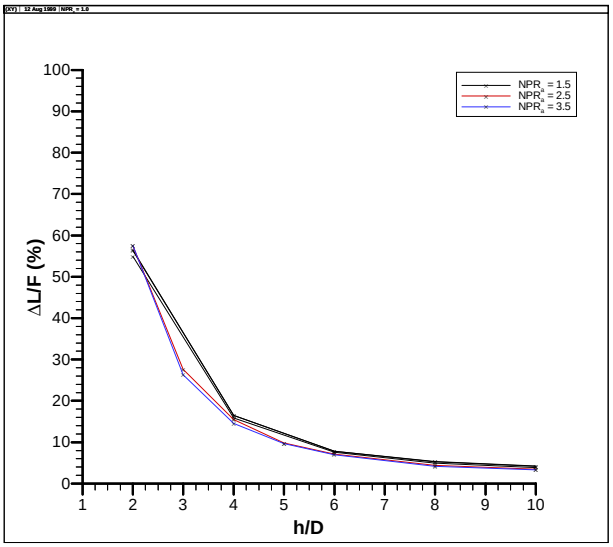

Fig. 15. Jet-induced suckdown (NPR$_c$ = 1.0).

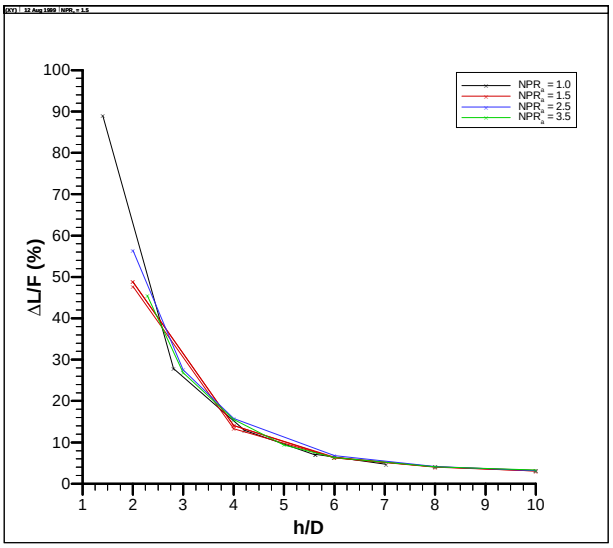

Fig. 16. Jet-induced suckdown (NPR$_c$ = 1.5).

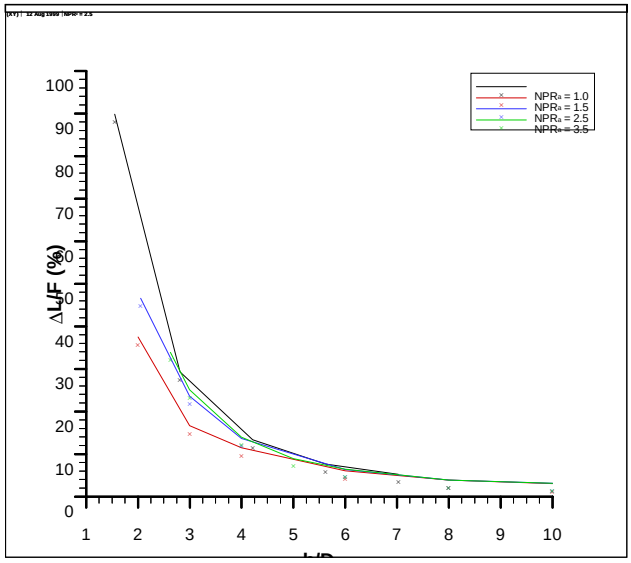

Fig. 17. Jet-induced suckdown (NPR$_c$ = 2.5).

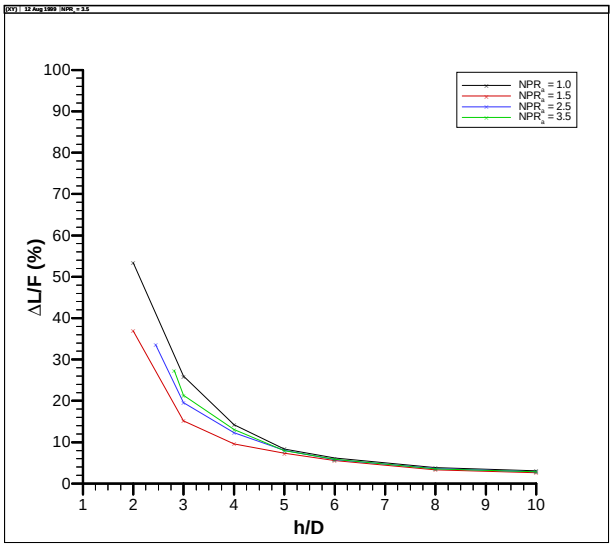

Fig. 18. Jet-induced suckdown (NPR$_c$ = 3.5).

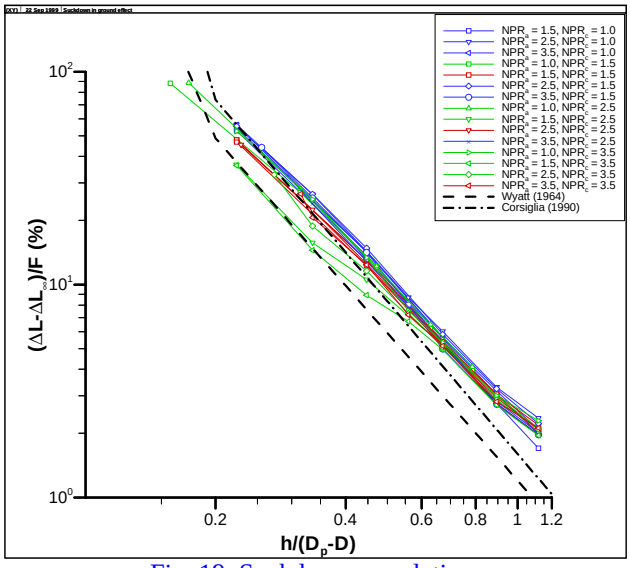

Fig. 19. Suckdown correlation.

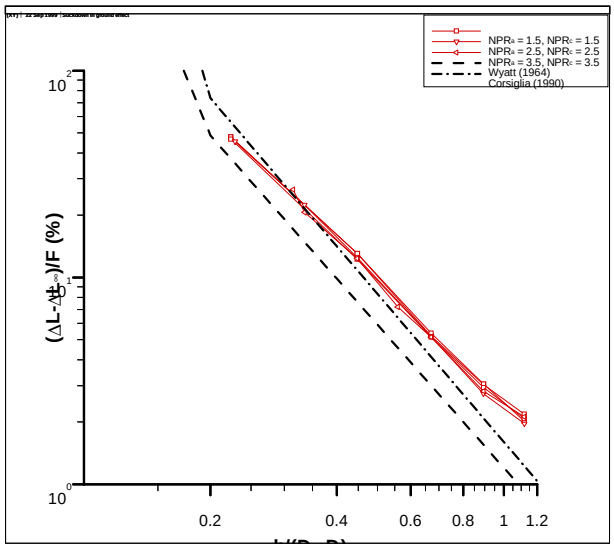

Fig. 20. Suckdown correlation (equal-NPR jets).

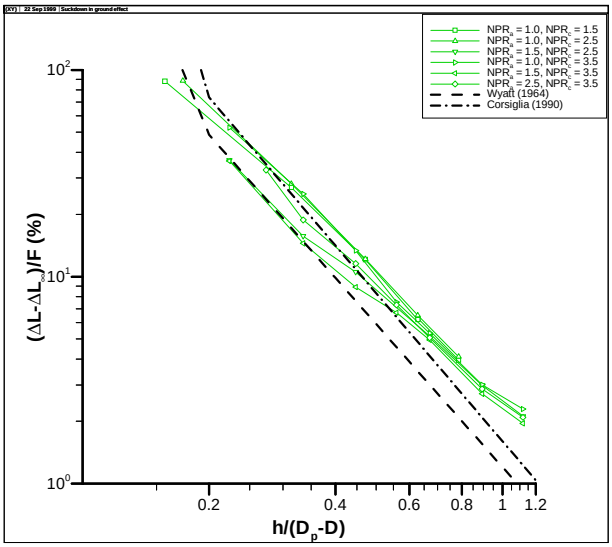

Fig. 21. Suckdown correlation (normal-profile jets).

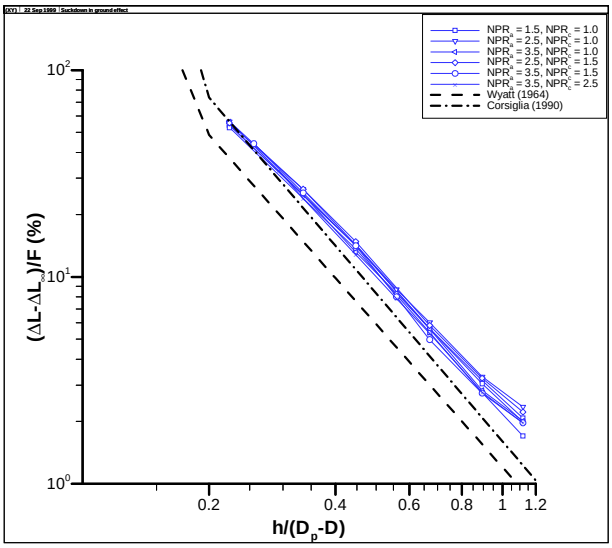

Fig. 22. Suckdown correlation (inverted-profile jets).